ELSEVIER

International Journal of Mass Spectrometry 215 (2002) 151–162

International Journal of Mass Spectrometry

www.elsevier.com/locate/ijms

Multi-hit, position-sensitive, time-of-flight spectrometry using a modified-backgammon-weighed-capacitor anode

F.A. Rajgara [a], D. Mathur [a,*], T. Nishide [b], T. Kitamura [b,1], H. Shiromaru [b], Y. Achiba [b], N. Kobayashi [b]

[a] *Tata Institute of Fundamental Research, Homi Bhabha Road, Mumbai 400 005, India*
[b] *Graduate School of Science, Tokyo Metropolitan University, Tokyo 192-0397, Japan*

Received 5 July 2001; accepted 30 October 2001

Abstract

A multi-hit, position-sensitive, time-of-flight measurement system using a two-dimensional position sensitive detector, which consists of a microchannel plate and a modified-backgammon-weighed-capacitor (MBWC) anode, was constructed for the study of dissociative ionization of highly-charged molecular ions produced in collisions of molecules with highly charged ions. The multi-hit capability of the detector enables event-by-event analysis. With the aid of multi-fold coincidence techniques, studies of the Coulomb explosion of multiply ionized triatomic molecules have been carried out by measuring the velocity components of all three ionic fragments produced in the fragmentation process. (Int J Mass Spectrom 215 (2002) 151–162) © 2002 Elsevier Science B.V. All rights reserved.

Keywords: Position sensitive detector; Time-of-flight spectrometry; Multiply charged molecules; Coulomb explosion

1. Introduction

Recent advances in the technology associated with position readout techniques in conjunction with developments of microchannel plate detectors with new types of anodes has enabled new insights to be gained into the complex dynamical properties of multiply charged molecules [1]. The use of time-of-flight (TOF) spectrometric techniques with position-sensitive detectors using different types of anode [2–7] make possible simultaneous detection, identification and analysis of more than one charged fragment that may be produced in the course of a single ion–molecule collision event. If the collision process involves a highly charged ion and a molecular target, multiple ionization of the target can occur. Molecules produced in high charge states are intrinsically unstable towards dissociation [1]. The velocity vectors of the ionic fragments that arise out of such dissociation can be determined from the measured position and TOF output from the position-sensitive detector. In addition to the kinetic energy release, which can be derived from conventional TOF measurements, event-by-event analysis of the type that becomes possible with new position-sensitive detector techniques gives deeper insight into the dynamics of the dissociation process and reveals the mechanisms involved in the interaction. From the angular correlation of the measured velocity vectors, it becomes possible to

* Corresponding author. E-mail: atmol1@tifr.res.in
[1] Present address: IBM Japan Ltd., Chou-ku, Tokyo.

1387-3806/02/$20.00
PII S1387-3806(01)00550-4

deduce hitherto-inaccessible structural information of the transition state, like the bond angle of molecular ion just prior to fragmentation.

By way of illustration of the potential that can be unleashed upon application of new detector technology to TOF spectrometry, we draw attention to a recent experiment in which the instantaneous chirality induced by zero-point molecular vibrations has been observed, for the first time [8]. To study such "burst" events, multi-hit capability is an indispensable feature of any position sensitive detector. This will be illustrated in the following. Additional features that are important in position-sensitive detectors's are high temporal and spatial resolution.

In the present paper, we present a detailed description of a new, position-sensitive, TOF spectrometry system that we have developed for studies of Coulomb explosions of triatomic and polyatomic molecular ions in high charge states. Such molecular states are accessed via collisions between a beam of highly charged atomic ions and neutral molecules. We also present details of the data analyzing procedure that we have developed in conjunction with our detector. We present some results of experiments that we have carried out on the Coulomb explosion of very highly charged states of the triatomic molecule, carbon disulphide.

2. The position sensitive detector system

2.1. Experimental apparatus

Before describing our new detector system, it is necessary to present an overview of the entire experimental apparatus into which the detector was incorporated. Our experiments were conducted using a crossed beams apparatus whose essential features are the following. A beam of highly charged ions (HCI) [Ar^{8+} at 120 keV] was produced using a 14.25 GHz, electron cyclotron resonance ion source (TMU-ECRIS). The extracted HCI beam was focussed by a three-element electrostatic einzel lens, analyzed by a sector magnet according to their mass to charge ratio, and transported to a collision chamber using a beam transport system comprising electrostatic steerers and deflectors. The mass-analyzed HCI beam was collimated using an aperture of 2 mm diameter and made to cross, at right angles, a molecular gas beam of CS_2 effusing through a multi-capillary plate. A turbo-molecular pump was used to base pressures of 6×10^{-9} Torr; typical working pressures were of the order of 8×10^{-7} Torr with CS_2 gas load. A more detailed description of the apparatus and methodology used is presented in a recent report [9].

In our experiments, multiple ionization of CS_2 occurred as a result of the interaction with the HCI beam. Fragment ions formed upon dissociation of highly-charged states of CS_2 were electrostatically deflected into a linear time-of-flight mass spectrometer (TOFMS) using an extraction field of 360 V cm^{-1} applied in a direction that was orthogonal to both the incident HCI beam and the target molecular beam. Auger electrons emitted by the projectile were detected by a channel electron multiplier, giving rise to fast timing pulses that served as a start trigger for our TOF measurements. The mass-to-charge analyzed fragment ions were detected by a 40 mm diameter microchannel plate detector coupled to a "modified backgammon with weighed coupling capacitors" (MBWC) anode. The anode divided the charge incident on it in terms of *x*- and *y*-coordinates in a manner that is described in the following. Some of our measurements, on the highest charge states, were also made with a 120 mm diameter microchannel plate detector.

2.2. The modified backgammon with weighed capacitors (MBWC) anode

A simple two-dimensional position readout technique using an MBWC anode, originally developed by Mizogawa and co-workers [10–12], was used by us to measure positions and times of flight of fragment ions produced upon dissociation of highly charged CS_2 molecular ions. The position readout anode possesses a wedge-and-strip configuration; it comprises a thin conductive layer divided into two regions by saw-teeth-like, narrow, insulating gaps. A schematic representation is depicted in Fig. 1.

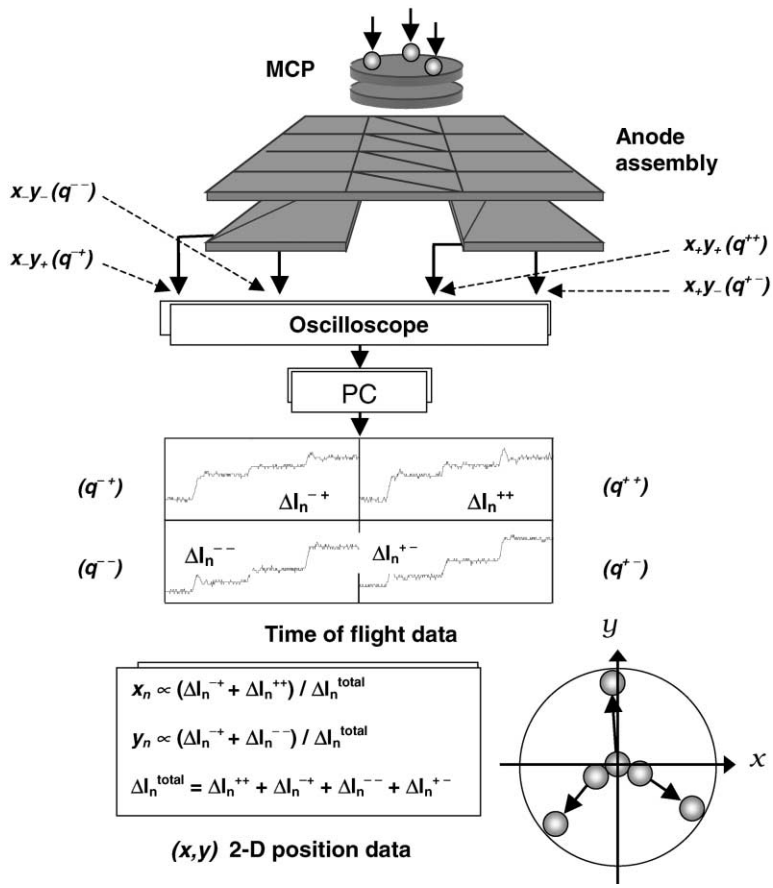

Fig. 1. A schematic representation of the detection system and procedure used in our experiments. A typical MBWC anode output, with three ions hitting within the same time window. Each step corresponds to the arrival of an ion. From the ratio of the four outputs for the each step, the position of each ion is determined and two-dimensional position data obtained (see text).

In general terms, the working principle of a position-sensitive detector such as ours is simple. A particle, or a photon, upon impinging on the front face of the two-stage MCP, gives rise to an avalanche of secondary electrons from the rear end of the MCP. This electron avalanche falls on the anode, and its spatial spread on the anode surface is generally wider than the repetition pitch of the wedge-shaped insulating lines. The charge is divided into two fractions by the insulating lines with a ratio that depends on the *x*-coordinate of the charge centroid. Each such fraction is transferred to charge dividers and further split into two fractions by capacitive couplings between the strips and the triangles, with a ratio that depends on the other, *y*-coordinate. Thus, four charge signals, q^{-+}, q^{++}, q^{--}, and q^{+-}, are extracted which, taken together, offer the possibility of obtaining two-dimensional position information. These position output signals, along with timing information, are fed to a four-channel digital storage oscilloscope after pre-amplification by charge-sensitive pre-amplifiers. The data are transferred to a computer via a GPIB bus. As explained later, the *x*-, *y*-position of each incident ion on the detector was determined from the relative heights of the pulses recorded on each channel.

Specific details of position-sensitive detector developed are as follows. It essentially consisted of a matched pair of microchannel plates, of 40 mm

diameter, in a chevron configuration. The MCP pair was followed by an MBWC anode, of dimensions 50 mm × 50 mm, with a wedge-and-strip pattern pitch of 2 mm and an insulating gap of 0.1 mm combined with the capacitive charge distributors. The MBWC anode was fully fabricated on a ceramic base for use in ultra high vacuum conditions. Typical values of position and timing resolution obtained using our MBWC anode were 200 μm and 2 ns, respectively.

The MBWC method is found to be free of thermal noise problems of the type that is sometimes of practical concern when other types of anodes are used. Of course, thermal noise generated within the MCP itself is unavoidable. On the other hand, we found that the MBWC method has the inherent disadvantage associated with the weighed coupling capacitor charge divider, which causes an increase of input capacitance for the preamplifier, thus, limiting the position resolution that may realistically be obtained. The response time of the detector, that is the time from avalanche creation to the signal output, is determined mainly by the preamplifier response time. The method adopted by us to extract time-of-flight information from raw data acquired on the detector is schematically indicated in Fig. 1.

2.3. TOF determination

A typical example of the MBWC output signal, as would be stored on the oscilloscope, as well as a schematic drawing of TOF profiling, are shown in Fig. 2. The output signals from the MBWC anode

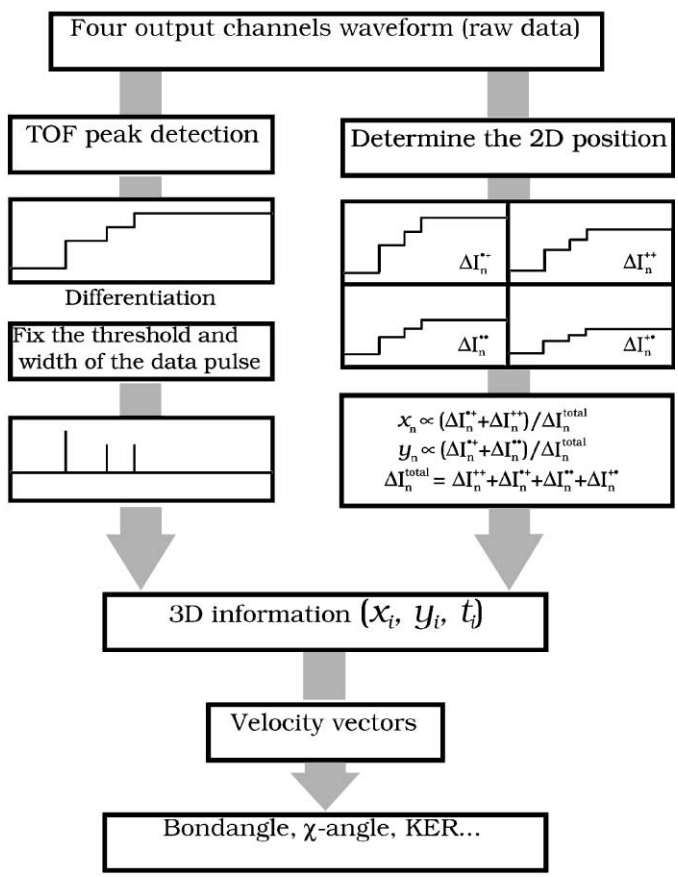

Fig. 2. Schematic representation of the analysis procedure used in the present experiments (see text).

would ideally be step functions, with each step corresponding to the arrival of specific ions. In other words, the TOFs of each fragment ions would be determined from the temporal position of the rising edge of the step signal. Thereafter, the procedure would be as follows. First, the four output step signals from the MBWC anode would be summed into one function. After that, in order to remove the effect of noise and ringing, a smoothing procedure in the data analysis program would be put into operation, resulting in a smoothed step function of the type shown in Fig. 3.

In order to make a precise temporal location of the rising edge of the signals, it might be considered natural to carry out differentiation of the step signal. Since the MBWC anode output is a fast rising step function, the peak of the derivative (above a suitably set threshold) corresponds to the TOF. The result obtained by such a differentiation and threshold method is considered by us to be reliable enough, except that sometimes consecutive step signals give rise to a certain amount of ringing after the first rising step signal. Such ringing may, at times, be detected as a real signal rising point, thus resulting in the TOF spectrum. This problem becomes even more serious when the two ions arrive at the detector within a short time period; under such circumstances, there is also a lowering of the accuracy of position determination. We found it important to take proper account of the number of steps, properly especially when larger polyatomic molecules are used as a target. A useful procedure that evolved in the course of our experiments is shown in Fig. 3.

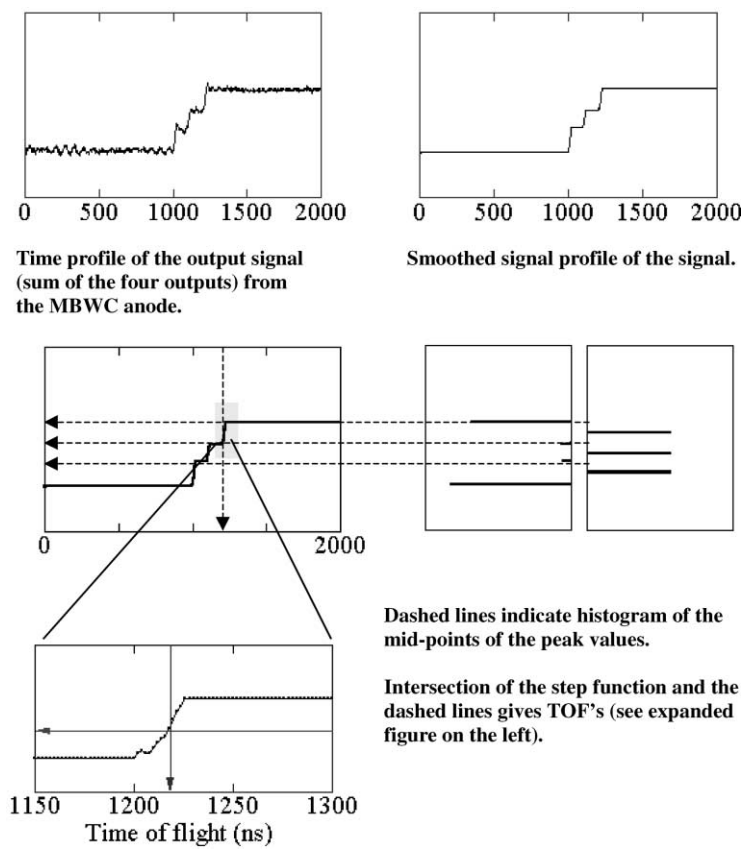

Fig. 3. Schematic representation of the smoothing TOF profiling procedure described in the text.

From the smoothed step function, a histogram of the voltage value is created and the peak of the histogram is detected. This procedure emulates a time-to-amplitude converter. The time t, which has a midpoint value of the step function, is determined. These values of t correspond to the arrival time of each fragment ion impinging on the detector input surface. We found the precision of TOF detection using this procedure to be better compared with the aforementioned differentiation method. This modification has also improved the positional resolution because the precision of determination of signal intensity is found to be better.

Technically, the signal step is a fast rising pulse, with a typical rise time of about 20 ns (see Fig. 3). Differentiation yields values of the steepest slope due to each rising time component. In case two ions arrive reach the detector within 20 ns (or less) of each other, the differentiation procedure yields the equivalent of a single hit. The step function procedure we adopt also has the same problem when two or more ions arrive within a short time interval. However, this method can, in principle, detect the baseline of the step function even if the time duration was only 2 ns.

Concerning multi-hit resolution, a compromise between positional and timing resolution is needed. In our present procedures, an event in which two ions hit the detector within 20 ns is excluded from further analysis, i.e. multi-hit resolution is set to 20 ns. If, in a given experiment, positional resolution is not considered to be too important, multi-hit resolution can be enhanced. Note that ion times of flight could routinely be determined using 2 ns time resolution (which also happened to be the temporal resolution of our digital oscilloscope).

2.4. Position determination

Typical examples of output waveforms obtained from our MBWC anode are shown in Fig. 1, with each step in the signal corresponding to the arrival of an ion. From the ratio of the four outputs for each step, the spatial position of each ion was determined as explained earlier. The four charge output signals, q^{-+}, q^{++}, q^{--} and q^{+-}, should have a ratio of the signal intensity according to the position in each step of signal. The TOFs have already been determined, as explained above. From each step height ΔI of the signals, as shown in Fig. 1, we can derive values of x_n and y_n in each TOF spectrum using:

$$x_n \propto \frac{\Delta I_{-/+} + \Delta I_{+/+}}{\Delta I_{\text{total}}},$$

$$y_n \propto \frac{\Delta I_{-/+} + \Delta I_{-/-}}{\Delta I_{\text{total}}},$$

$$\Delta I_{\text{total}} = \Delta I_{2+} + \Delta I_{-/+} + \Delta I_{-/-} + \Delta I_{+/-}.$$

We note that since the vertical resolution of the oscilloscope is eight-bit, the estimated resolution of 200 μm is much larger than the intrinsic positional resolution of the MBWC anode.

3. Some typical results and analysis

3.1. Time and position measurements

The results that we report here concern the dissociation process that occurs when a CS_2 molecule interacts with Ar^{8+} ions. We focus attention on the Coulomb explosion of the highly charged $CS_2{}^{q+}$ ($q = 3$–10) ion that is formed in this interaction and we monitor those dissociation channels that result in three fragment ions. An example of one such interaction is:

$$Ar^{8+} + CS_2 \rightarrow CS_2{}^{3+} \rightarrow S^+ + C^+ + S^+.$$

We recorded the spatial positions (x_i, y_i) and flight time (t_i) of all the three fragment ions relative to the start electron. If the number of ions detected by a single trigger is less than three, then those data are not analyzed. The x-, y-position of each incident ion was determined from the relative heights of the pulses recorded on each channel.

In our experiments, we found that the x, y image obtained on the periphery of the MCP was slightly deformed. Although this did not induce any obvious (visible) distortion of the derived velocity vectors, we took the precaution of excluding all ion signals that were

detected in the peripheral 1.5 mm area of our MCP in order to avoid possible systematic error in the results discussed later in this paper. Moreover, as stated above, some of the measurements were also repeated using a larger, 120 mm diameter detector. In addition to this, the yields of some dissociation channels were underestimated due to a limitation of detection efficiency arising from the following factor. Although the time resolution of the measurement system was 2 ns, if two ions were to hit the detector within very short time difference, the positional accuracy would be lowered. To avoid possible systematic error, the events in which two ions hit within 20 ns were, therefore, excluded from further analysis. This discrimination is particularly of importance when, for instance, the charge state of the two S-ions is the same, or in cases where the dissociation events involve S^{3+} ($m/z = 10.7$) and C^+ ($m/z = 12$) coincidences [i.e. the (3, 1, 3) channel]. We took special care (as indicated later) in determinations of yields of these dissociation channels while selecting close lying overlapping regions for $S_b{}^{3+}$ and C^+ ions from the coincidence map while analyzing the data. Thus, in TOF spectra in Fig. 4, besides C^+ ions there is a contribution of $S_b{}^{3+}$ ions in the same region, though not specifically labeled in the spectra.

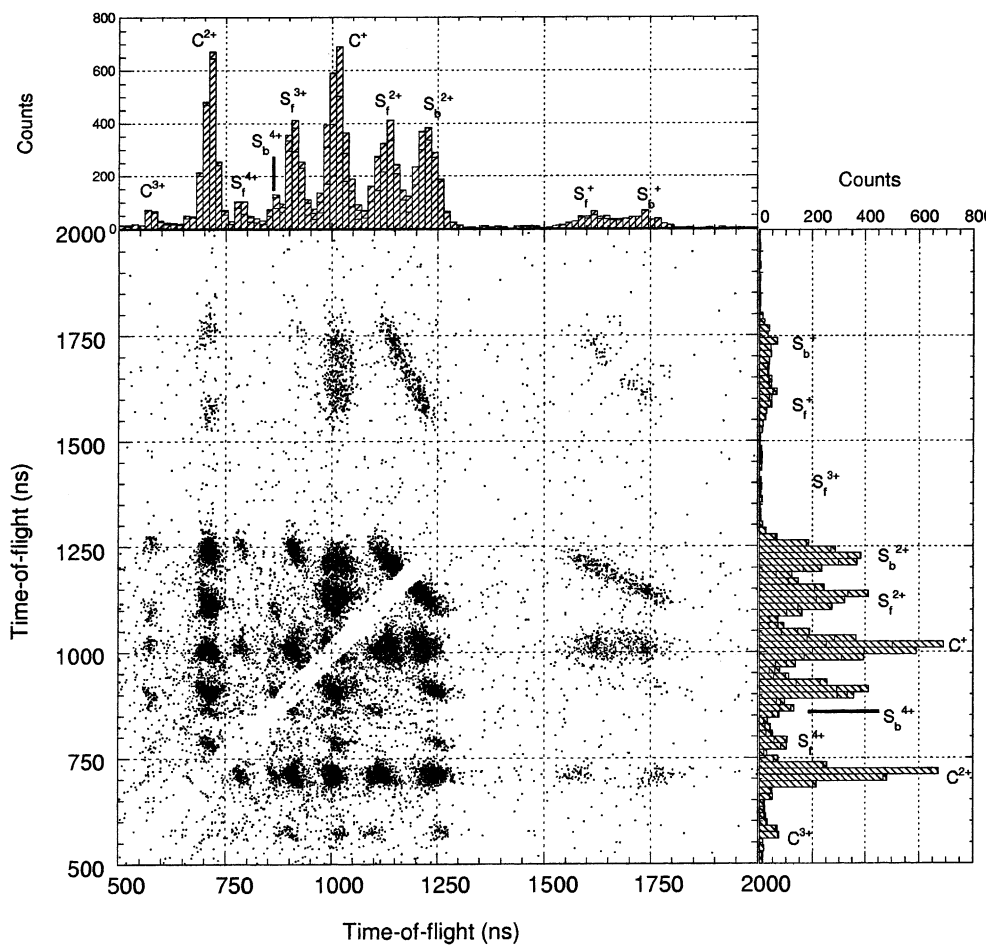

Fig. 4. Triple coincidence map and time-of-flight spectrum of fragment ions produced in collisions of Ar^{8+} with CS_2. The C^+ peak also contains a small contribution from $S_b{}^{3+}$ fragment ions (see text).

3.2. Three-dimensional velocity vector determinations

The measured positions and flight times of the fragment ions (x, y, t) enabled us to generate three dimensional initial velocity vectors using the following methodology. The triple coincidence signals of the fragment ions (comprising electron–ion–ion–ion signals) were assigned to the corresponding dissociation channels of CS_2^{q+} (q = 3–10). From the TOFs of each of the fragment ions, the z-components of the velocity vectors were determined: the position information yielded x- and y-components of the velocity vector for each fragment ion formed in a single dissociation event. Hence, it is straightforward to determine the velocity components (v_x, v_y, v_z). An example of the determination procedure in the case of a triatomic molecule is as follows. From values of (x_n, y_n, t_n) and fragment ion mass m_n where n = 1–3, supposing that (x_{mc}, y_{mc}) is a coordinate of the molecule's center-of-mass, then,

$$v_{nx} = \frac{x_n - x_{mc}}{t_n},$$

$$v_{ny} = \frac{y_n - y_{mc}}{t_n},$$

$$\sum m_n v_{nx} = \sum m_n v_{ny} = 0.$$

As a result, v_{nx} and v_{ny} can be determined using these relations. Next, the z-component of the velocity vector, v_{nz}, is determined from the TOF of each fragment. Since the components of initial velocity originate from a Coulomb explosion, that gives rise to considerable kinetic energies (at least greater than 1–2 eV [1]), it is not unnatural to neglect the initial translational velocity of the molecule (which is essentially due to thermal energy). A table of the v_z values is constructed. These values depend both on the initial position (center-of-mass) and the flight time t. To be specific, the procedure adopted by us to calculate the v_z table is as follows: (i) the z-coordinate of center-of-mass, mc_z, is fixed to some position on the TOF axis in the collision volume; (ii) while changing the v_z value within a given range, the TOF is calculated; (iii) from the different mc_z values, step (ii) is executed again, so that mc_z values cover the entire range of the collision volume; (iv) steps (i) to (iii) are repeated for each mass of the fragment ions, and as a result, a functional table of v_{nz} (t_n, mc_z) is created. Referring to this table, satisfying momentum conservation, and keeping position of the mc_z constant for all the fragments, we can then deduce the z-velocity component v_{nz}.

Using this procedure, the three-dimensional velocity vectors of each fragment ions (v_{nx}, v_{ny}, v_{nz}) can be determined from the experimental dataset (x_n, y_n, t_n).

3.3. Coincidence maps

Fig. 4 shows a typical coincidence map measured in our experiments. Maintaining very low count rates (less than one count per second for triple coincidence events, whereas total ion count rates may be few hundreds per second) minimizes the possibility of false coincidences. Each point in the map is due to a coincidence signal of three ions. The density of points that give rise to dark patches, or islands, represent different fragmentation channels as different highly charged CS_2^{q+} (q = 3–10) ions that are formed in the HCI–CS_2 interaction break-up. Fig. 4 also shows conventional TOF spectra of the fragment ions.

In order to illustrate the type of information that such coincidence maps yield, we consider the way to deduce the information due to the (a, b, c) channel where the notation a, b, c indicates the dissociation channels of CS_2^{q+} breaking into S^{a+}, C^{b+} and S^{c+}, with $q = a + b + c$. For a specific (2, 2, 2) channel consider the region of the map in the vicinity of the temporal region corresponding to the C^{2+} fragment. The spectrum that results is depicted in Fig. 5a and shows sulfur ions (in different charge states) that are formed in coincidence with the C^{2+} fragment; these represent the (a, 2, c) dissociation channel, where a, c = 1–4. For each charge state there are two peaks that are denoted by subscripts 'f' and 'b', representing respectively those fragment ions that were ejected in an initial direction toward, and away from, the detector (corresponding to "forward" and "backward"

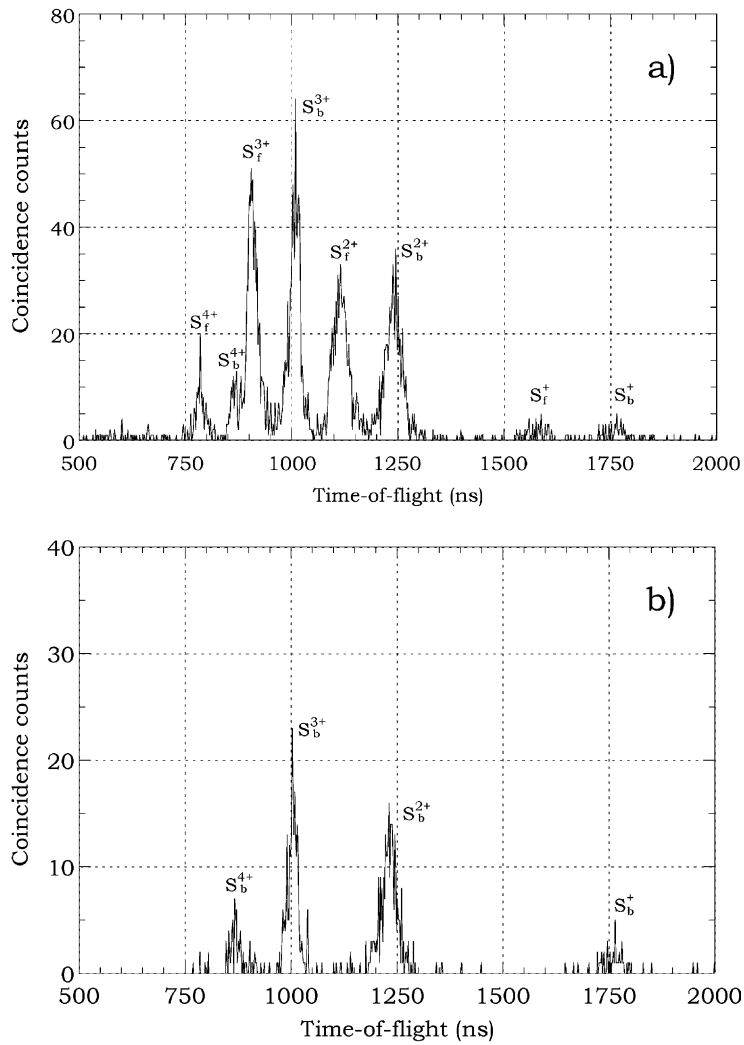

Fig. 5. TOF spectrum of fragments ions produced (a) in coincidence with C^{2+} and then (b) in coincidence with C^{2+} and $S_f{}^{2+}$.

scattered ions in collision physics parlance). It should be noted that the absence of signals between the forward and backward was due to the fact that we excluded the event in which two S^{2+} ions arrived at the detector within 20 ns. Choosing subsets of specific channels carried out further reduction of data. For instance, Fig. 5b shows the spectrum of those ions that are also produced in coincidence with the $S_f{}^{2+}$ fragment, yielding the (2, 2, c) channel, where $c = 1$–4. The specific (2, 2, 2) channel was then obtained from the points under the $S_b{}^{2+}$ ion in Fig. 5b. The kinetic energy of all the ions in the fragmentation event were obtained by summing $(mv^2)/2$ for (x, y, z) components, and the total kinetic energy released in the break-up of the molecular ion was obtained for each charge state of the molecular ion. We note that the data do not show "forward" and "backward" splitting in the case of C^{q+} ions, indicating that very little energy is imparted to the central carbon nucleus in the fragmentation process.

3.4. Bond angle and χ-angle

The angular correlation between the fragment ions may be expressed in terms of the χ-angle, which is the angle between the velocity vector of the central C-ion and the difference between the velocity vectors of the two S-ions. We also explored the possibility that it might be possible to gain some insight into whether the dissociation mechanism involving highly charged molecular ions CS_2^{q+} ($q = 3$–10) is sequential or simultaneous by probing the distribution of χ-angles as a function of ion yield. The χ-angle was calculated according to the formula

$$\cos(\chi) = \frac{\boldsymbol{v}_{\mathrm{c}} \cdot (\boldsymbol{v}_{\mathrm{s1}} - \boldsymbol{v}_{\mathrm{s2}})}{|\boldsymbol{v}_{\mathrm{c}}| \times |(\boldsymbol{v}_{\mathrm{s1}} - \boldsymbol{v}_{\mathrm{s2}})|}$$

where $\boldsymbol{v}_{\mathrm{c}}$, $\boldsymbol{v}_{\mathrm{s1}}$, and $\boldsymbol{v}_{\mathrm{s2}}$ are the unit vectors along the dissociating carbon and two sulfur ions, respectively. Physically, the χ-angle indicates the direction of the outgoing carbon with respect to the line joining the S–S nuclei.

We further probed the nuclear geometry of the dissociating molecular ion by reconstructing the S–C–S angle θ_0 from the trajectories of the fragment ions for a single identified dissociation channel. Firstly, the angle θ_{v} between the velocity vectors of the two outgoing S-ions was calculated using the formula

$$\cos\theta_{\mathrm{v}} = \frac{\boldsymbol{v}_{\mathrm{s1}} \cdot \boldsymbol{v}_{\mathrm{s2}}}{|\boldsymbol{v}_{\mathrm{s1}}| \cdot |\boldsymbol{v}_{\mathrm{s2}}|}$$

and, then deducing the bond angle by comparing with simulated data obtained in terms of a plot of angle θ_{v} against the θ_0.

Fig. 6a shows histograms depicting the measured bond angle distributions for the (2, 2, 2) and (3, 1, 2) fragmentation channels, respectively. Also shown are computed bond angle distributions (solid line) obtained assuming a purely Coulombic fragmentation, with the zero-point vibration of the degenerate bending mode taken into account. The fact that the experimentally determined distributions of bond angle closely follow those predicted from the zero-point vibration of the neutral molecule indicates strongly that the fragmentation occurs instantly in a non-sequential manner. The fragment velocities show a dependence on the measured bond angle, which is in good agreement with the Coulomb theory.

Fig. 6b shows histograms depicting the measured χ-angle distributions for the (2, 2, 2) and (3, 2, 1) fragmentation channels. As is seen the χ-angle values for the symmetric dissociating channels has the most probable value close to 90°. This again confirms our postulate that the fragmentation is instantaneous, and non-sequential processes appear to be important in the fragmentation dynamics of CS_2^{q+} ($q = 3$–10) ions. It was also observed that the probable values of the χ-angle for all the dissociation channels, the χ-angle values for the asymmetric product channels are larger than 90°, which is expected from the fragmentation of a bent molecular systems with different recoil velocities.

We recall that while analyzing some specific dissociation channels that involve overlapping fragment ion peaks, special care had to be taken to ensure that the experimentally observed bond angle distribution does not deviate from the computed bond angle distribution. At times one can also see repetitive peaks in the experimental bond angle distribution when selection of dissociation fragment channels is not done properly. Similar deviations can also be seen in the χ-angle distributions under such circumstances. In this respect, measurements of bond and χ-angle distributions also served as a useful diagnostic for us.

3.5. Fragment ion kinetic energy release

The measured velocity vectors have been used to deduce the fragments kinetic energy release (KER) and hence the total KER released in the fragmentation of the CS_2^{q+} ($q = 3$–10) molecular ion. Measured KER values as shown in Fig. 6c were found to be more or less the same as those predicted by a pure Coulombic explosion, revealing the apparent unimportance of binding electronic interactions in multi-electron systems in high charge states [9]. *Ab initio* quantum computations were carried out to calculate KER values for different fragmentation processes. The calculation was to the lowest possible electronic states of a given charge state and represented the lower limit to the

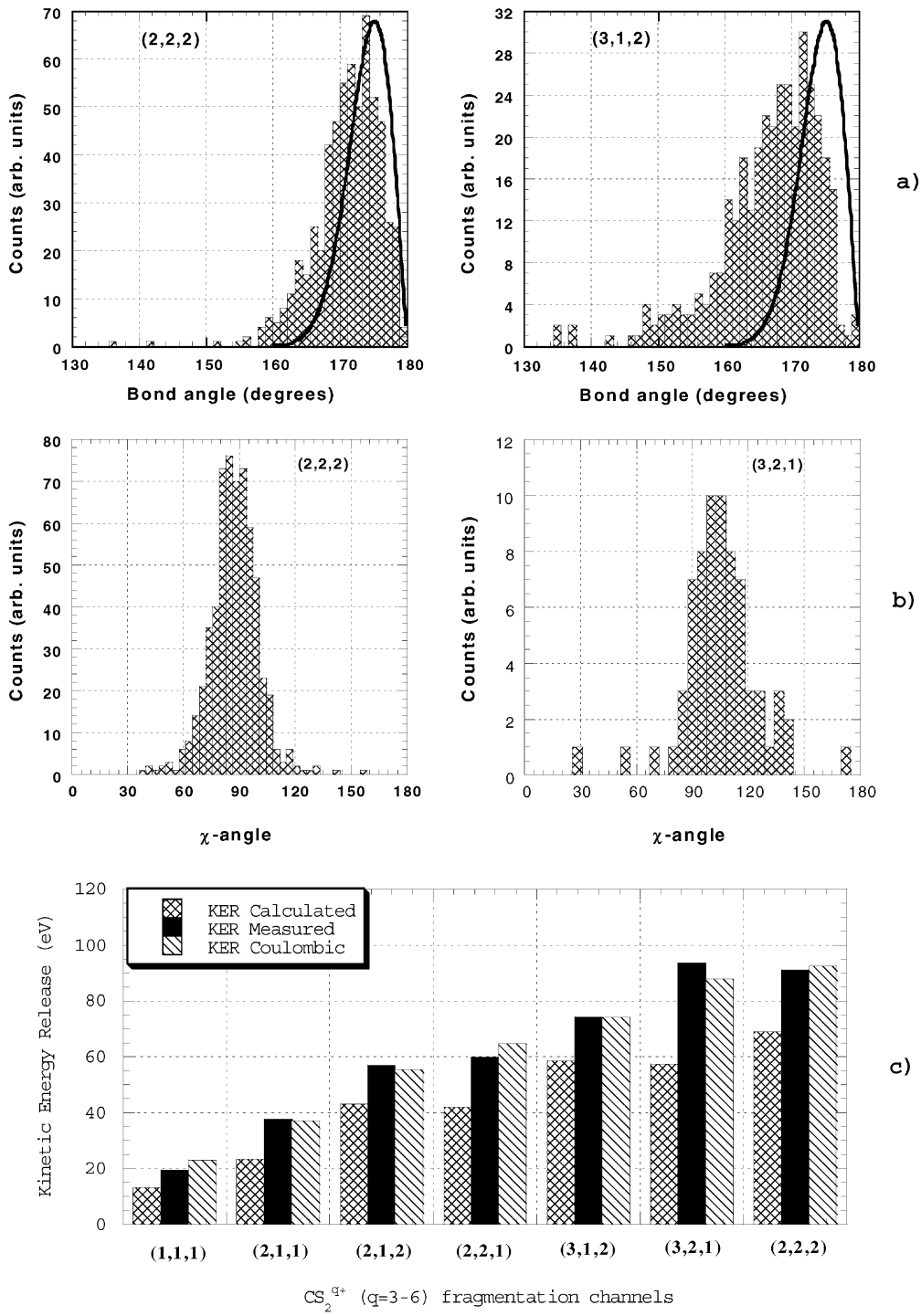

Fig. 6. (a) Histogram of bond angle distribution for the (2, 2, 2) and (3, 1, 2) channels. (b) Histogram of χ-angle distribution for (2, 2, 2) and (3, 2, 1) channels. (c) Comparison of kinetic energy release values for dissociating CS_2^{q+} molecular ion upto charge 6+.

expected values. These calculated values were found to be lower than the experimental values, and demonstrate the importance of electronic excitation of the precursor molecular ions produced in fragmentation process.

4. Conclusions

A new position sensitive detector system using an MBWC anode that we have incorporated into a coincidence time-of-flight spectrometer has been described. Experiments indicate a satisfactory linear image over the full effective area, except for a small peripheral area (of radius 1.5 mm) where fringing fields from the applied voltages might lead to some measure of image distortion. The imaging procedure that we have developed yields new information on the fragmentation dynamics following Coulomb explosion of multiply charged molecular ions. Specific examples have been given on determination of important and hitherto-inaccessible molecular structure parameters, such as bond angle and kinetic energy release values.

Acknowledgements

The Japanese Society for the Promotion of Science as well as the Department of Science and Technology, Government of India, are thanked for support of this collaborative research through the RONPAKU program.

References

[1] D. Mathur, Phys. Rep. 225 (1993) 193.
[2] D.P. de Bruijn, J. Los, Rev. Sci. Instr. 53 (1982) 1020.
[3] A. Fabis, W. Koenig, E.P. Kanter, Z. Vager, Nucl. Instrum. Methods B 13 (1986) 673.
[4] A. Belkacem, A. Fabis, E.P. Kanter, W. Koenig, R.E. Mitchelle, Z. Vager, B.J. Zabransky, Rev. Sci. Instr. 61 (1990) 946.
[5] J. Becker, K. Beckord, U. Werner, H.O. Lutz, Nucl. Instrum. Methods A 337 (1994) 409.
[6] J.A. Schultz, S. Ulrich, L. Woolverton, W. Burton, K. Waters, C. Klein, H. Wollnik, Nucl. Instr. Methods 118 (1996) 758.
[7] J. Ullrich, R. Moshammer, R. Dörner, O. Jagutzki, V. Mergel, H. Schmidt-Böcking, L. Spielberger, J. Phys. B 30 (1997) 2917.
[8] T. Kitamura, T. Nishide, H. Shiromaru, Y. Achiba, N. Kobayashi, J. Chem. Phys. 115 (2001) 5.
[9] F.A. Rajgara, M. Krishnamurthy, D. Mathur, T. Nishide, T. Kitamura, H. Shiromaru, Y. Achiba, N. Kobayashi, Phys. Rev. A 64 (2001) 032712.
[10] T. Mizogawa, Y. Awaya, Y. Isozumi, R. Katano, S. Ito, N. Maeda, Nucl. Instrum. Methods A 312 (1992) 547.
[11] T. Mizogawa, M. Sato, Y. Awaya, Nucl. Instrum. Methods A 366 (1995) 129.
[12] T. Mizogawa, M. Sato, M. Yoshino, Y. Itoh, Y. Awaya, Nucl. Instrum. Methods A 387 (1997) 395.